Electronic Supplementary Material for

Response of rangeland vegetation to snow cover dynamics in Nepal Trans Himalaya

Climatic Change

Keshav Prasad Paudel and Peter Andersen

Department of Geography, University of Bergen, Fosswinkelsgate 6, N-5007 Bergen, Norway

Corresponding Author:

K. P. Paudel
Tel. : +47 98683685
fax: +4755583089
e-mail: keshav.paudel@geog.uib.no

This PDF file includes:

Supplemental material:

Data and preprocessing

We used 228 Moderate Resolution Imaging Spectroradiometer (MODIS) Terra 16-day composite NDVI images with 250 m spatial resolution (MOD13Q1 – version 005) and corresponding pixel reliability data, spanning the period from 2000 to 2009. The study area lies within MODIS tile H25V06. We used the MODIS Reprojection Tool (MRT, 2008) to project MODIS images from the native sinusoidal projection into the Universal Transverse Mercator (UTM) projection and to convert the image to GEOTIFF format.

The MODIS NDVI products are composited over the 16 day period with the Constrained View Angle Maximum Value Composite (CV-MVC) and/or the MVC algorithm to generate a higher quality, cloud free, and near nadir observations composite NDVI (Didan and Huete, 2006; Solano et al., 2010). However, significant residual effects remain in some of the 16-day NDVI composites due to atmospheric conditions such as cloud cover, ozone, dust and other aerosol effects (Holben, 1986). Such atmospheric "noise" in the NDVI value needs to be corrected. In addition, the effect of presence of snow and melt complicates the use of NDVI time series for computing vegetation phenological metrics in snow affected areas (Beck et al., 2006) since the snow cover has a negative effect on the NDVI and the snow melt causes NDVI value to rise without being related to increased vegetation activity. Such influences of snow cover and melt on NDVI value need to be corrected.

Negative bias in NDVI values caused by snow cover was corrected by following the procedure of Beck et al. (2006; 2007). With this aim, we first selected NDVI values > 0 recorded in snow free conditions during December 19 to March 20 (six NDVI observations from Julian day 353 of the previous year to Julian day 65 of the current year). The presence of snow and ice was derived directly from MODIS snow cover data. We then computed the $NDVI_w$ of each pixel as the mean of the minimum NDVI selected for each snow season. Next, we replaced all NDVI values in the snow covered pixel by $NDVI_w$ of the given pixel. In order to correct for noise in the NDVI value caused by cloud and other atmospheric conditions, we used the Iterative interpolation for cloud-free Data Reconstruction (IDR) methodology (Julien and Sobrino, 2010) which includes the following four steps: a) extraction of time series NDVI values for each pixel; b) computation of an alternative NDVI value for each date as the mean of the immediately preeceding and following days observation; c) replacement of NDVI value in the original time series with the alternative time series NDVI value when the pixel reliability value in the QA data set was other than 0 (good data) and the maximum difference between both time series is higher than 0.02 NDVI units, and d) iteration of the above three steps until convergence is reached.

We used snow cover duration data (500 m resolution) for the period 2000 – 2009 computed from the daily MODIS snow cover products with removal of cloud obscuration (Paudel and Andersen, 2011). We extracted the dates of first snow accumulation and last snow melt for each pixel of each snow season.

Three meterological stations (Fig. 1) provided daily temperature data of the period 1970 – 2008. Daily precipitation data from 13 stations within the area were also collected.

References

Beck P, Atzberger C, Høgda K, Johansen B, Skidmore A (2006) Improved monitoring of vegetation dynamics at very high latitudes: A new method using MODIS NDVI. Remote Sensing of Environment 100:321-334.

Beck P, Jönsson P, Høgda KA, Karlsen SR, Eklundh L, Skidmore AK (2007) A ground-validated NDVI dataset for monitoring vegetation dynamics and mapping phenology in Fennoscandia and the Kola peninsula. International Journal of Remote Sensing 28:4311-4330.

Didan K, Huete A (2006) MODIS vegetation index product series collection 5 change summary. In: The University of Arizona. http://landweb.nascom.nasa.gov/QA_WWW/forPage/MOD13_VI_C5_Changes_Document_06_28_06.pdf.

Holben BN (1986) Characteristics of maximum-value composite images from temporal AVHRR data. International Journal of Remote Sensing 7:1417-1434.

Julien Y, Sobrino JA (2010) Comparison of cloud-reconstruction methods for time series of composite NDVI data. Remote Sensing of Environment 114:618-625.

MODIS Reprojection Tool (MRT) (2008) User's Manual, Release 4.0. In: Land Processes DAAC USGS EROS Center in Collaboration with Department of Mathematics and Computer Science, South Dakota

School of Mines and Technology. https://lpdaac.usgs.gov/lpdaac/content/.../MRT_Users_Manual.pdf.

Paudel KP, Andersen P (2011) Monitoring snow cover variability in an agropastoral area in the Trans Himalayan region of Nepal using MODIS data with improved cloud removal methodology. Remote Sensing of Environment 115:1234-1246.

Solano R, Didan K, Jacobson A, Huete A (2010) MODIS vegetation indices (MOD13) C5 user's guide. In: Terrestrial Biophysics and Remote Sensing Lab, The University of Arizona. <http://tbrs.arizona.edu/project/MODIS/UsersGuide.pdf>

Supplemental material:

Characterization of rangeland phenology

Figure 2 shows regional maps of mean and corresponding trend of onset, end and length of the growing season during the time period analyzed. The decadal mean and trend of time of peak NDVI value, time of maximum NDVI, and time integrated annual (ΣNDVI) and pre-monsoon NDVI are shown in Figure S1. The figures show very high spatial variability of phenological dates as well as vegetation production across the study area which was primarily correlated to moisture regime and associated altitudinal variation. The average peak and start date of the growing season have a similar spatial pattern and generally increase from low to high altitude in lower Mustang, lower Manang, upper Manang and Nar Phu regions (Fig 2a and S1a). In the drier upper Mustang the average SOS occurred relatively late. In contrast, the mean date of the EOS generally increased from high to low altitude except in the Nar Phu region where the average EOS occurred earlier. Local altitudinal variations in snow cover pattern and surface temperature are the main reasons proposed for this progression. Annual maximum NDVI ($NDVI_{max}$) value as well as time integrated annual and pre-monsoon NDVI follow the same spatial pattern of moisture regimes and/or snow cover duration.

The correlation analysis between $NDVI_{max}$ and $\Sigma A2J_{ndvi}$ over the study area by year shows $r^2 > 0.62$ (average $r^2 = 0.69$), similarly the coefficient of determinant between $\Sigma A2J_{ndvi}$ and ΣNDVI is greater than 0.94 (average $r^2 = 0.96$) and that between ΣNDVI and $NDVI_{max}$ is greater than 0.79 (with average $r^2 = 0.83$). A pixel-wise correlation analysis between ΣNDVI and $NDVI_{max}$ over the last decade shows that 70 % of rangeland pixels have a $r^2 > 0.5$ and 70% of the rangeland areas reveal a strong positive correlation ($r^2 > 0.4$) between pre-monsoon and annual accumulated NDVI.

One of the striking features observed in the region was the substantial decline in annual maximum NDVI, ΣNDVI and $\Sigma A2J_{ndvi}$ in semi arid zones (upper Mustang, upper Manang and Nar Phu). In contrast, most of the areas in the less dry zones (lower Manang and lower Mustang) had increasing or relatively stable vegetation production in terms of annual maximum, pre-monsoon and annual NDVI (Fig S1). A pixel-wise linear trend analysis of $NDVI_{max}$ shows that about 71% of the study area has a declining trend (Fig.S1e). However, only 50.2% pixels with a declining trend are statistically significant (Fig. S1f). About 60% of the study area has a declining trend in terms of ΣNDVI , of which 37% pixels are statistically significant (Figs. S1h, S1i). About 3% of the area has a significant positive trend in $NDVI_{max}$, and 10% area in time integrated annaul NDVI has a significant positive trend ($p<0.1$).

The interannual mean and standard deviation of growing season parameters for different zones are summarized in Table S1. The mean SOS occurred between 1 June and 11 July in 61% of the study area. In more than 72% of the study area, the average peak and end of season occurred during the month of August and October respectively. The mean onset date of green-up in upper parts of the study area in both semi arid and arid climatic eco-zones was delayed, while in southern lower eco-zones, in the transition between tropical humid alpine and arid climate zones, has advanced over the last decade (Fig. 2b). Generally, LGS in the semi arid areas has declined, while it has increased in lower Manang, lower Mustang and Nar Phu during the study period. The spatial pattern of change is more sporadic than continuous, however. About 57.3% of the area was found to have a declining trend in LGS in the last decade. Only 8.5% of the study area showed a statistically significant positive trend in LGS over the last decade (Figs. 2h, 2i).

A pixel-wise correlation analysis over the last decade shows that LGS was strongly correlated with SOS ($r = 0.81$, $p< 0.0001$) but relatively less correlated with EOS ($r = 0.62$, $p< 0.0001$). Similarly, average time of peak NDVI over the Trans Himalayan rangeland was found to be strongly correlated with average SOS ($r = 0.76$, $p = 0.011$). These suggest that interannual variations in rangeland LGS and time of peak NDVI are mostly due to interannual variation in SOS.

Table S1: Average growing season parameters for various zones

Zones	Onset date (SOS)		Peak date		End date (EOS)		Length (LGS)	
	Mean	S.D.	Mean	S.D.	Mean	S.D.	Mean	S.D.
Upper Mustang	25 June	16.01	11 Aug	14.08	11 Oct	13.4	108 days	22.1
Lower Mustang	14 June	23.8	10 Aug	17.7	14 Oct	13.8	123 days	27.4
Upper Manang	10 June	20.7	7 Aug	13.9	13 Oct	14.3	126 days	27.5
Nar Phu	17 June	12.1	6 Aug	9.7	30 Sep	10.9	106 days	15.5
Lower Manang	28 June	23.5	18 Aug	14.4	20 Oct	13.3	116 days	28.1
Study area (average)	22 June	19.7	11 Aug	13.9	12 Oct	13.1	113 days	24.1

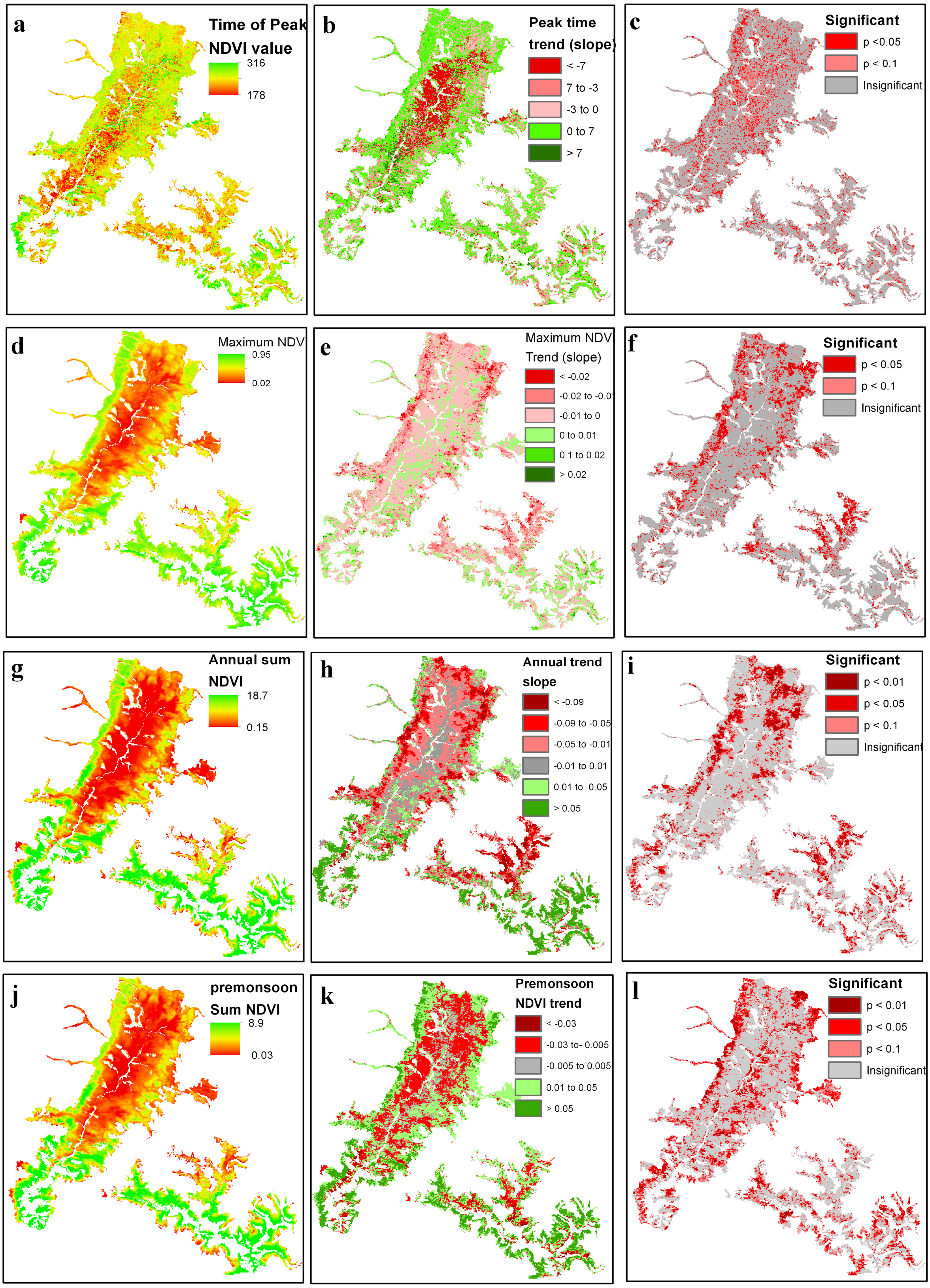

Fig. S1 Regional maps of average time of peak NDVI, annual maximum NDVI value, annual sum NDVI and pre-monsoon sum NDVI (a, d, g, j), their respective trends (b, e, h, k) and significance of trend (c, f, i,l) over the last decade. Trends are termed insignificant for pixels in which p> 0.1